J Nanostruct 15(3): 1333-1345, Summer 2025

RESEARCH PAPER

Development of $CeVO_4$/rGO Nanocomposite via Sonochemical Synthesis for High-Capacity Electrochemical Hydrogen Storage

Mahsa Rezayeenik [1], *Mehdi Mousavi-Kamazani* [1]*, *Sahar Zinatloo-Ajabshir* [2]*

[1] *Department of Nanotechnology, Faculty of New Sciences and Technologies, Semnan University, Semnan, Iran*

[2] *Department of Chemical Engineering, University of Bonab, Bonab, Iran*

ARTICLE INFO

Article History:
Received 05 April 2025
Accepted 27 June 2025
Published 01 July 2025

Keywords:
$CeVO_4$/rGO
Electrochemical
Hydrogen storage
Nanocomposite
Sonochemical

ABSTRACT

One of the effective methods for storing hydrogen in solid form is electrochemical storage, which is performed under ambient temperature and pressure conditions. This method especially provides stable and effective performance for porous materials. In this research, using hydrazine as a new reactant, $CeVO_4$/rGO nanocomposite was fabricated via one-step sonochemical approach. With the help of hydrazine, not only the unwanted growth of cerium vanadate nanoparticles was limited, but also the possibility of one-step synthesis and reduction of graphene oxide (GO) to reduced graphene oxide (rGO) was easily provided. The obtained nanocomposite was analyzed by EDS, BET, FTIR, XRD, and FESEM. Also, the FESEM images confirm that the fine rod nanoparticles were formed using ultrasonic radiation and dispersed on the wrinkled sheets of reduced graphene oxide in one step. $CeVO_4$/rGO nanocomposite was utilized for the electrochemical hydrogen storage by the chronopotentiometry method. The discharge capacity of $CeVO_4$/rGO nanocomposite was nearly 4929 mAh/g, that is remarkable compared to the storage capacity of $CeVO_4$ nanoparticles (4087 mAh/g).

How to cite this article
*Rezayeenik M., Mousavi-Kamazani M., *, Zinatloo-Ajabshir S. Development of $CeVO_4$/rGO Nanocomposite via Sonochemical Synthesis for High-Capacity Electrochemical Hydrogen Storage. J Nanostruct, 2025; 15(3):1333-1345. DOI: 10.22052/JNS.2025.03.049*

INTRODUCTION

With the emergence and prominence of consequences resulting from excessive human use of fossil fuels, coupled with the knowledge that we will face a shortage of these fuels in the not-so-distant future, we are far from achieving global energy security [1-3]. Recently, the consequences of these predictions have prompted governments to dedicate a significant portion of their investment and research to the production and storage of safe and desirable clean energy. Consequently, proposed plans to provide energy through clean energy are frequently expressed and compared. As a result, these comparisons and experiments by researchers continuously refine methods, and modern approaches are also being developed [4-8]. Due to its unique features and potential to provide energy security, hydrogen is considered by scientists as the basis for the next generation of future energy systems and a promising alternative to today's fossil fuels [9-13]. Currently, hydrogen production is possible and sustainable using three methods: fossil fuels (non-renewable sources), renewable sources, and electrochemical methods [14-19]. By purposefully choosing a method of

* *Corresponding Authors Email: M.Mousavi@semnan.ac.ir*
s.zinatloo@gmail.com

storing and transporting hydrogen, based on the materials used, we can maximize its potential [8, 16, 20-22]. One promising method is the electrochemical storage of hydrogen, which has garnered significant attention due to its reversibility and the low operating temperature and pressure associated with the hydrogen absorption process in electrode materials [15, 16, 23]. In addition, the physical absorption of hydrogen is quickly reversible, and its enthalpy is lower than that of chemical absorption; this lower enthalpy helps reduce thermal control problems [23]. Because hydrogen storage is primarily based on chemical or physical surface absorption, the specific surface area and porosity of materials are the most critical parameters affecting absorption [15, 16]. Nanomaterials play a great role in hydrogen storage as the latest material tailoring technique due to their sole properties [12, 24]. Many types of research have been studied to identify suitable materials for hydrogen storage, including carbon nanotubes (CNTs), nanocomposites, metal-organic frameworks (MOFs), etc [25]. Hydrogen storage in solid materials and room conditions with complete safety has now been extended to hydrogen storage [16, 26 ,27]. The chronopotentiometry method is a three-electrode technique that is performed by applying current. Among the important groups of inorganic nanomaterials, $CeVO_4$ from infrequent earth vanadate families has been extensively evaluated owing to its magnetic features, great electronic conductivity properties,

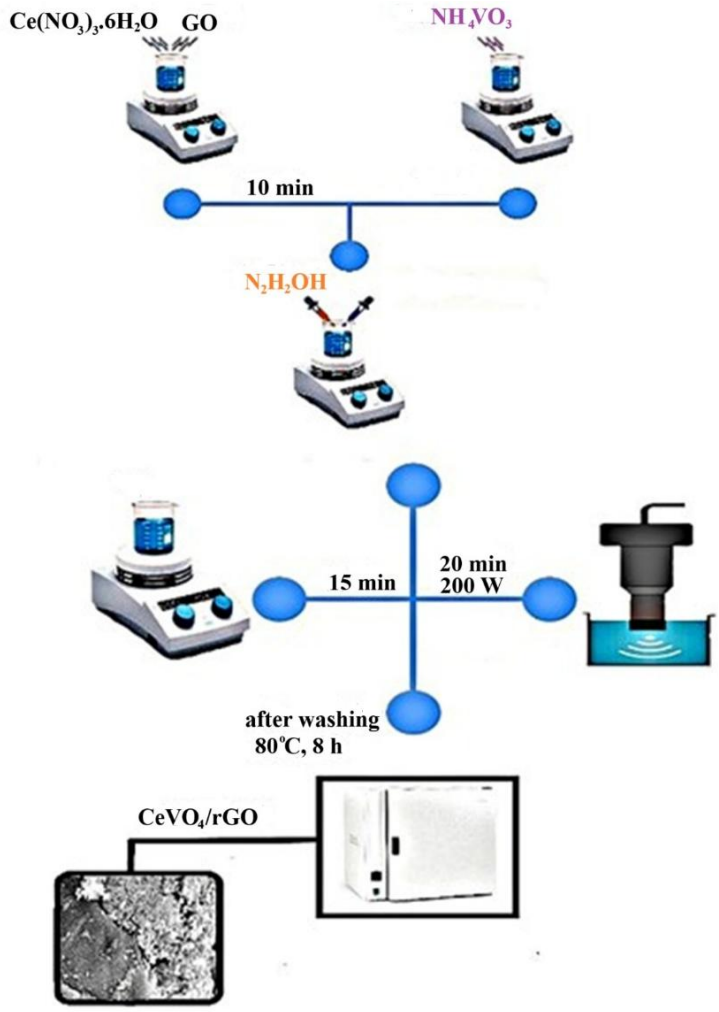

Fig. 1 Synthesis steps of $CeVO_4$/rGO nanocomposite.

proper specific surface area, and suitable electrochemical performance [12]. The suitable and porous composite structure of this material with substances like graphene oxide and graphite, it has significantly improved its performance. However, rGO with improved electrochemical properties as well as layered structure is suitable as an improved substrate for nanoparticles and increased efficiency and ease of storage [28]. The effect of rGO in increasing hydrogen storage can be seen in the works of researchers such as Valian et al. with the synthesis of new $Li_{0.35}La_{0.55}TiO_3$/rGO nanocomposite and Guemou et al. who introduced a novel rGO-supported Ni-Nb nanocomposite observed [8, 29]. The sonochemical process that has benefited from green chemistry by displaying the attractive morphology of regular particle size and also creating more surface area is one of the simplest and most efficient methods that has been noticed in recent years for the synthesis of inorganic nanomaterials [30]. In our previous work [12], we synthesized $CeVO_4$/rGO nanocomposite through hydrothermal method and investigated its performance in hydrogen storage, which was

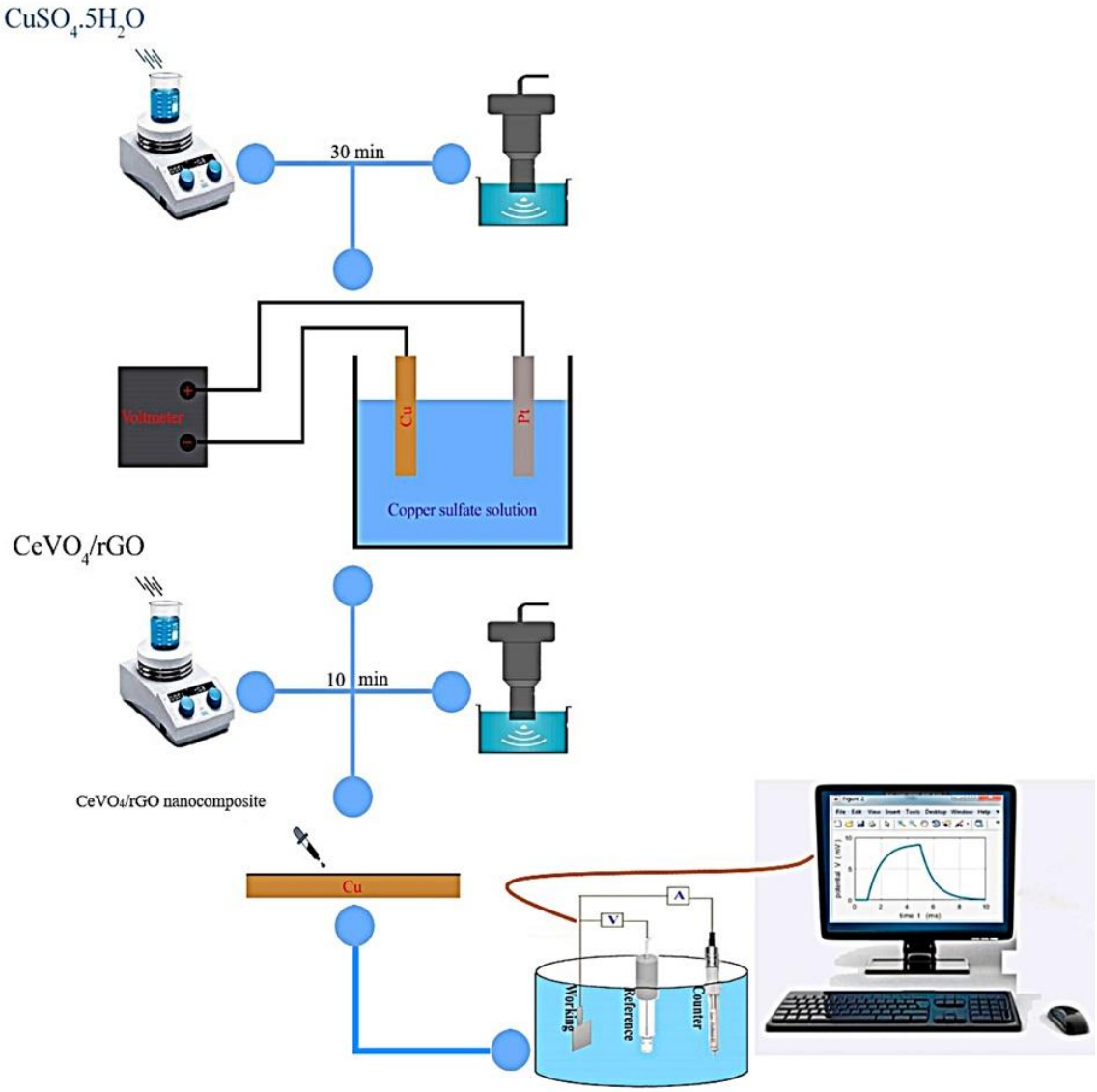

Fig. 2 The steps of electrochemical hydrogen storage by $CeVO_4$/rGO nanocomposite.

very favorable. Again, we believe that more work can be done about this composite. Therefore, here, in order to improve the storage efficiency, we synthesized $CeVO_4$/rGO nanocomposite by a one-step sonochemical method as a simpler and faster method in the synthesis of high surface area nanomaterials. From hydrazine as a reduction factor GO to rGO, it enables rGO to perform one -step synthesis. Finally, the performance of the $CeVO_4$/rGO nanocomposite was investigated by EDS, FTIR, XRD, BET, and FESEM analysis for hydrogen storing through an electrochemical process.

MATERIALS AND METHODS

Materials and instruments

Hydrochloric acid (HCl), ammonium metavanadate (NH_4VO_3), graphite, cerium (III) nitrate hexahydrate ($Ce(NO_3)_3{\cdot}6H_2O$), potassium hydroxide (KOH), $KMnO_4$ (potassium permanganate), H_2SO_4 (sulfuric acid), H_2O_2 (hydrogen peroxide), and hydrazinium hydroxide (N_2H_2OH) without any further purification from Merck were procured and used. Fourier Transform Infrared Spectrometer analysis was done utilizing Magna-IR, spectrometer 550 550 Nicolet with a resolution of 0.125 cm in KBr pellets in the range of 400--4000 cm^{-1}. FESEM images were recorded by MIRA3 FEGSEM. By Philips-X 'PertPro device using Ni-filtered Cu Kα radiation, X-ray diffraction patterns were prepared. A Philips XL30 microscope device was used to perform energy dispersion spectroscopy (EDS) analysis. BJH analysis was done to explore the specific surface area and pore size distribution. N_2 adsorption/desorption (BET) analysis was obtained utilizing a Belsorp-mini device. Ultrasonic waves were produced using a 20 kHz ultrasonic device with a maximum output power of 400 watts and a probe (APU500) diameter of 12 mm.

Synthesis of $CeVO_4$/rGO nanocomposite

GO was fabricated from graphite by the Hammers approach [31]. The first solution was prepared by dissolving 0.43 g of $Ce(NO_3)_3{\cdot}6H_2O$ and 0.1 g of GO in 24 ml of distilled water. Then, 0.116

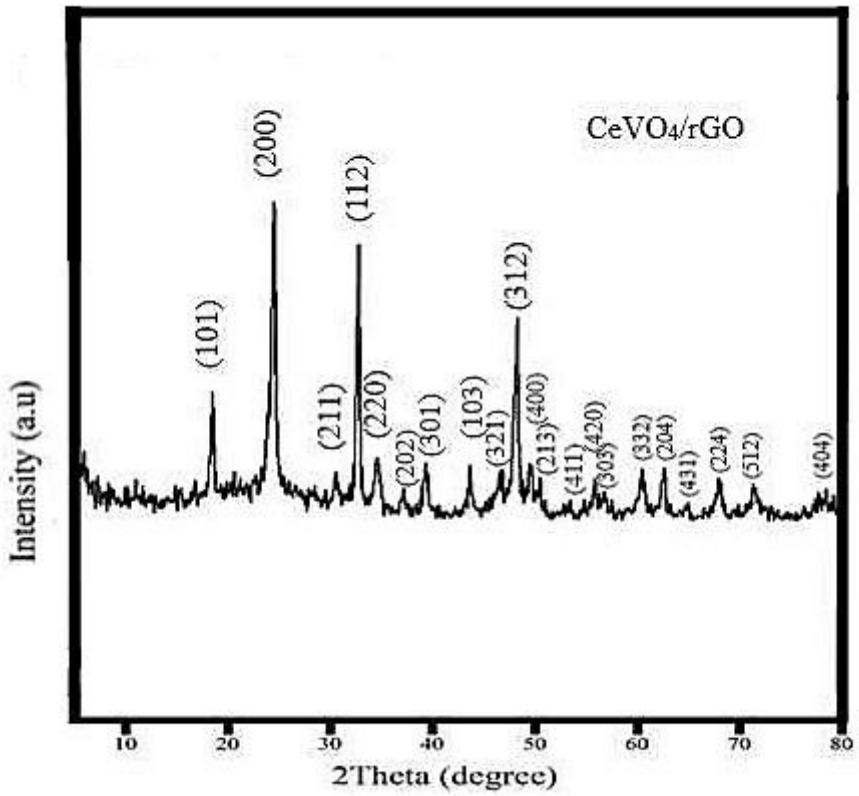

Fig. 3. XRD pattern of the as-synthesized $CeVO_4$/rGO nanocomposite.

g of ammonium metavanadate (NH_4VO_3) has been dissolved in 24 ml of distilled water (secondary solution). The secondary solution was slowly added into the first solution while stirring. Then 8 ml of

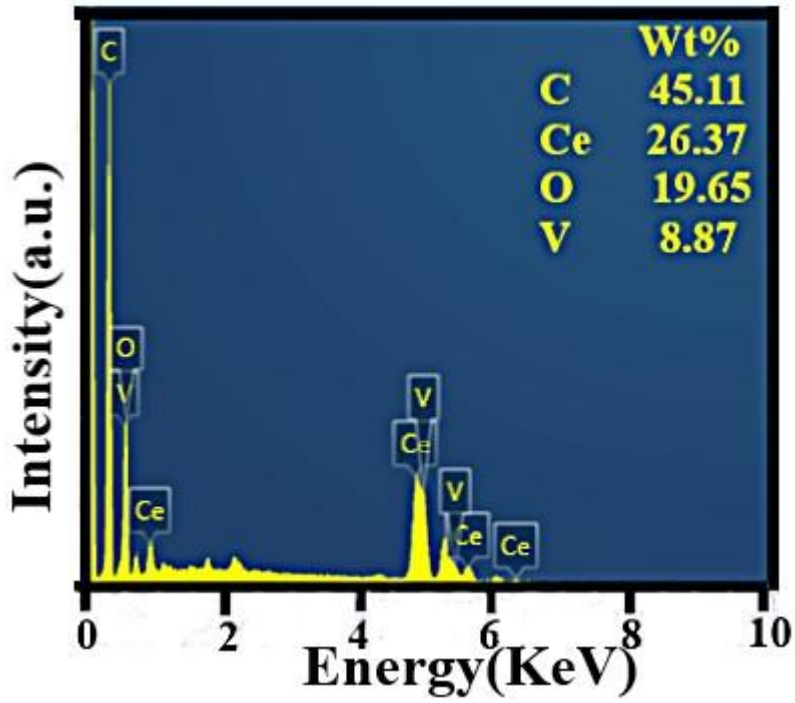

Fig. 4. EDS spectrum of the as-synthesized $CeVO_4$/rGO nanocomposite.

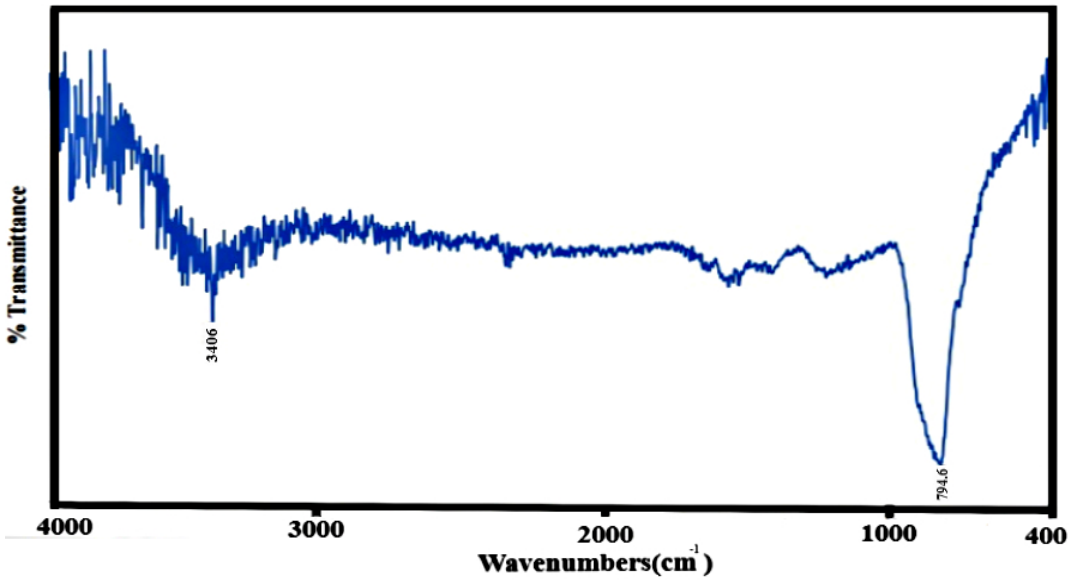

Fig. 5. FT-IR spectrum of the as-synthesized $CeVO_4$/rGO nanocomposite.

distilled water and 2 ml of hydrazine were added into the mentioned solution, and also stirred on a heater within 15 minutes. Finally, ultrasonic was performed with a power of 200 watts in one step and for 20 minutes. The synthesis steps are shown in Fig. 1. The storage capability of synthesized $CeVO_4$/rGO nanocomposite was investigated by chrono-potentiometric approach in the presence of three electrodes, working electrode, reference electrode (Ag/AgCl), and counter electrode (Pt) in potassium hydroxide (KOH) solution. [30]. Fig. 2 shows the steps of electrochemical hydrogen storage.

RESULTS AND DISCUSSION

The XRD data of $CeVO_4$/rGO nanocomposite is presented in Fig. 3. The absence of a signal at an angle of $2\theta \approx 10.6°$ reveals that GO is reduced [32]. The XRD pattern of Fig. 3 shows the tetragonal structure of $CeVO_4$ (JCPDS = 120757) with lattice parameters a = 7.39 Å, b = 7.39 Å, and c = 6.48 Å. The EDS data of $CeVO_4$/rGO nanocomposite is displayed in Fig. 4. Only V, Ce, O, and C signals can be apperceived in the EDS spectrum. Besides, there are no other impurities, and it is consistent with the XRD findings. To investigate the organic groups and chemical bonds of $CeVO_4$/rGO nanocomposites, FT-IR spectroscopy is presented in Fig. 5. The signal at 794 cm^{-1} is assigned to asymmetric stretching vibrations of V-O [33]. The asymmetric stretching and bending vibration of the O-H bond in several signals near 3400 cm^{-1} and 1640 cm^{-1} is caused by H_2O molecules adsorbed upon the external surface of $CeVO_4$/rGO nanocomposites [34]. The conversion of graphene oxide to reduced graphene oxide can be confirmed by the absence of C=O as well as C-O-H bond peaks that emerge around 1715 cm^{-1} and also 1400 cm^{-1}, correspondingly [35]. Fig. 6 is related to the FESEM data with different magnifications of the as-synthesized $CeVO_4$/rGO nanocomposite. As can be seen, rod-like $CeVO_4$ nanoparticles with an approximate diameter of 10 nm and a length of about 20 nm are spread on the graphene sheets. One of the characteristics of the formation of smaller particles size that leads to superior performance in hydrogen adsorption is the creation of a higher specific

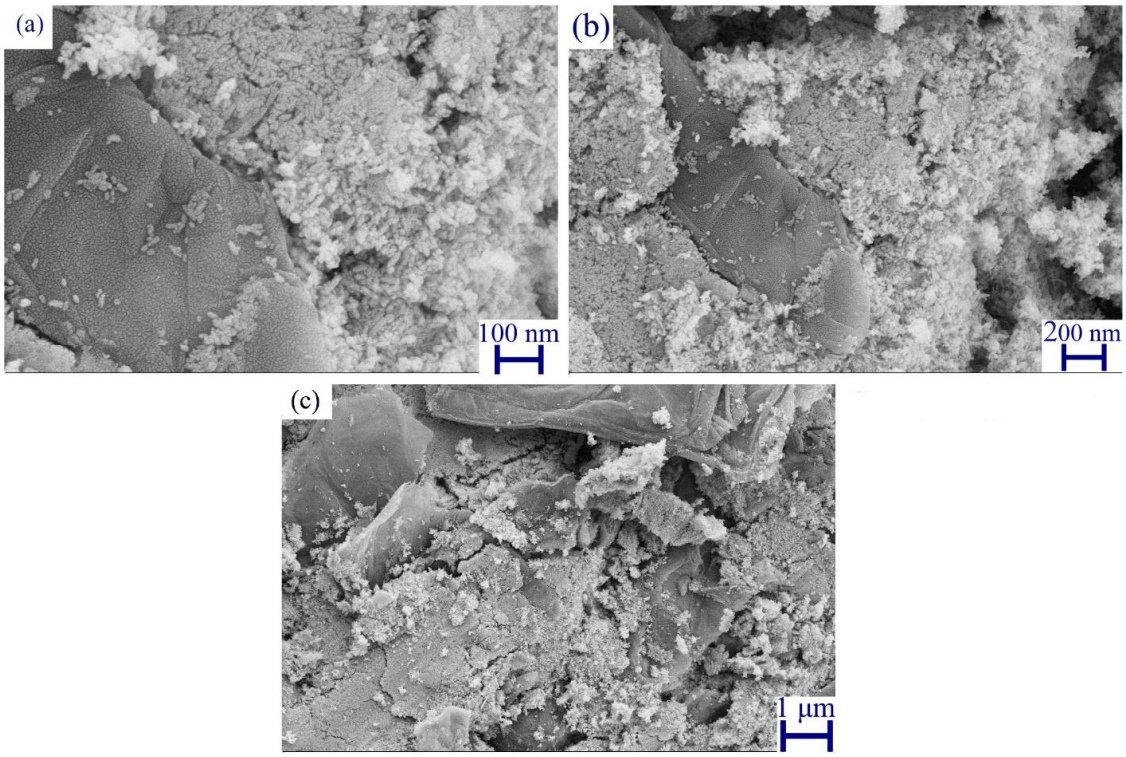

Fig. 6. FESEM images of the as-synthesized $CeVO_4$/rGO nanocomposite.

surface. One of the most key features of materials and nanocomposites to be suitable candidates for hydrogen storage is having a proper specific surface area and favorable porosity. In general, the amount of gas adsorbed on the adsorbent can be related to its surface area. The BET analysis in Fig. 7 displays the N_2 adsorption/desorption isotherm as well as the pore size distribution of the synthesized nanocomposite using the Bart Joyner Holland (BJH) method. The isotherm observed in Fig. 7a corresponds to the type IV isotherm with H3 type residual loops, that represent mesoporous and solid particles with porous nature [36]. These residual loops are created in sheet-like structures and stacked compounds that do not show limiting absorption at high p/p_0 [37-39]. Furthermore, the pore size distribution (BJH) in Fig. 7b confirms the meso-porosity of the sample. As can be seen in Fig. 7a, this isotherm has a hysteresis in the relative pressure between 0.7-1, which is a high relative pressure, the absorption increases and the holes are filled [40]. Also, the presence of hysteresis indicates the presence of hollow structures in the synthesized nanocomposite [41], which is consistent with SEM observations (Fig. 6). Specific area (a_s), total pore volume (V_t), and also mean pore diameter (D_m) for the synthesized nanocomposite are: 60.342 m^2g^{-1}, 0.11294cm^3g^{-1}, and 8.5773 nm, respectively. In general, with the increase of the specific surface area of the nanocomposite, the amount of storage capacity increases because more surface area (a_s) can create more active storage sites.

Electrochemical Hydrogen Storage Tests

Cyclic voltammograms of the synthesized nanomaterials, pure oxide nanostructure and the prepared nanocomposite were examined in the 2 molar potassium hydroxide electrolyte [42]. The cyclic voltammetry experiments were also performed with scan rate of 0.1 V/s [42]. The CV results of the two investigated nanostructure samples are depicted in Fig. 8. As can be seen, both samples prepared as electrode compounds for hydrogen storage exhibit the reversible curve in the potential range of -1 to -0.2 V. Table 1 gives the anodic and cathodic feedback information. It is clear that the anodic and cathodic currents of the nanocomposite sample are greater than the pure oxide nanostructure, which can demonstrate its better electrochemical features for energy storage [43]. It has been accepted that the presence of graphene-based compounds can have a positive effect on improving the electrochemical characteristics of nanomaterials owing to their favorable conductivity and proper structural properties [42]. In addition, the anodic and cathodic signals appearing in the CV curves denote the reversible adsorption/desorption process as well as adsorption of hydrogen upon the electrode

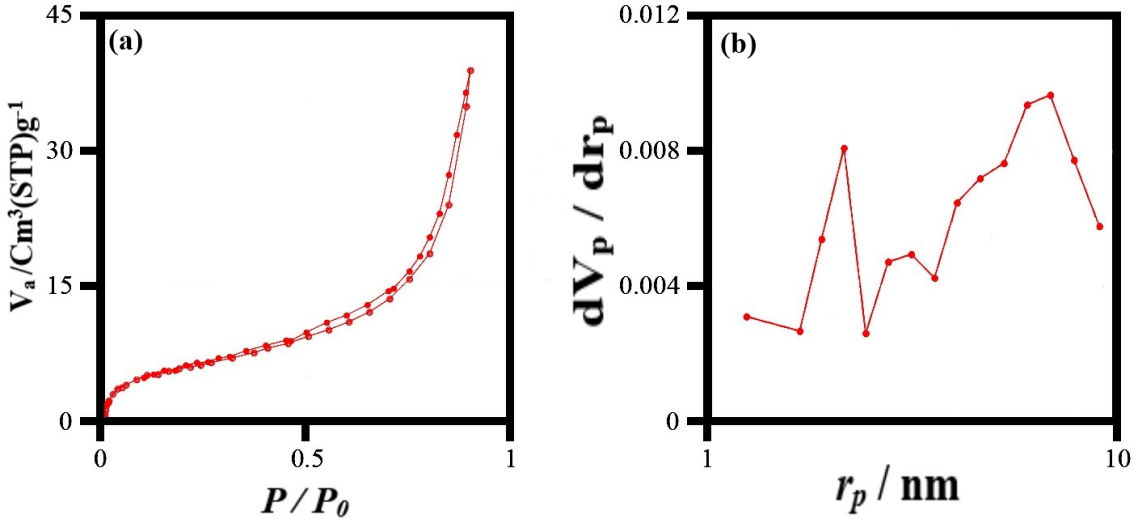

Fig. 7. N_2 adsorption/desorption isotherms and BJH pore size distribution of $CeVO_4$/rGO nanocomposite.

surface, correspondingly [42, 43].

In this experimental work, the chrono-potentiometric approach was applied to measure and compare the hydrogen adsorption and desorption capacity of the synthesized nanomaterials, pure oxide nanostructure and the prepared nanocomposite (see Figs. 9 and 10). It has been reported that during the adsorption process, a number of water molecules in the electrolyte can be decomposed in the vicinity of the working electrode [43, 44]. H species in the electrolyte may be either adsorbed on the nanostructures coated on the working electrode or recombined on the electrode surface, leading to the formation of hydrogen molecules. These molecules will disperse on the electrode or create gas bubbles upon the electrode surface [43, 44]. It is worth noting that with the continuation of this process, the voltage can enhance and the adsorption in the nanostructures can continue. It has been reported that during the deposition step, the hydrogen species released from the nanostructures can combine with the hydroxyl species in the alkaline electrolyte and lead to the formation of water molecules. The reactions that can perform in these two stages are [16, 44, 45]:

$$ge^- + \text{Nanostructure} + gH_2O \rightarrow gOH^- + (gH + \text{Nanostructure})$$

$$(gH + \text{Nanostructure}) + gOH^- \rightarrow ge^- + \text{Nanostructure} + gH_2O$$

In order to check and measure the values of adsorption and desorption capacity, a constant current (one milliampere) is employed to start the process of hydrogen adsorption in nanostructures. As the process of hydrogen adsorption continues, the voltage can enhance. It has been observed that when the adsorption curve is flat, H species

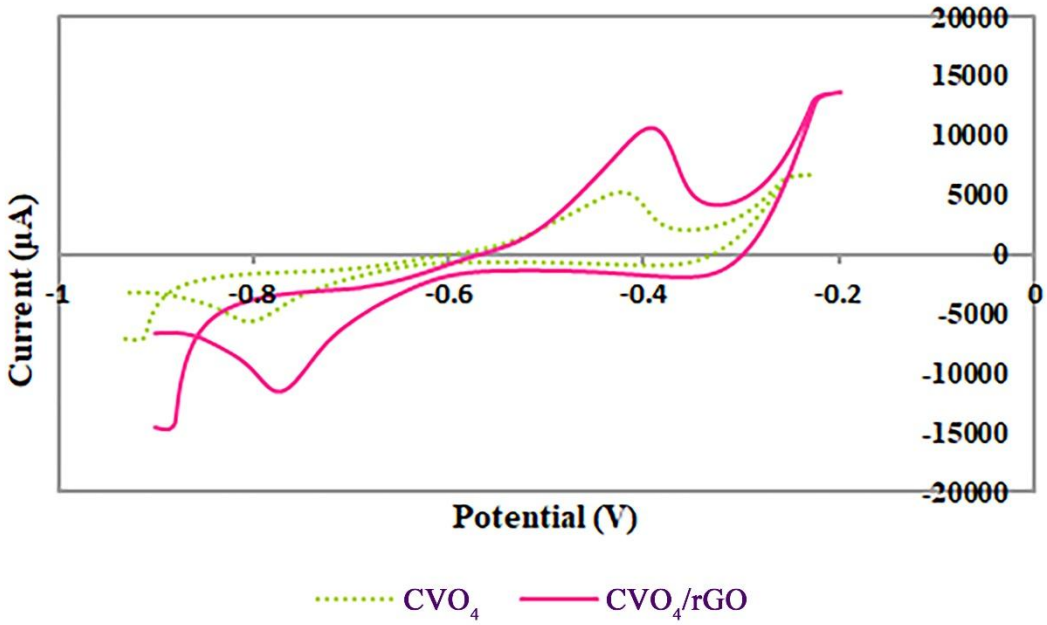

Fig. 8. Cyclic voltammograms for as-fabricated samples.

Table 1. Electrochemical parameters of the as-synthesized samples for CV.

Electrode	I_{Pa} (µA)	I_{Pc}(µA)	E_{Pa} (V)	E_{Pc} (V)
$CeVO_4$ nanostructure	5087	-5474	-0.414	-0.798
$CeVO_4$/rGO nanocomposite	10533	-11442	-0.387	-0.769

can be completely adsorbed upon the working electrode [16, 25, 44]. In this project, in order to explore the impact of rGO on the electrochemical storage capacity of the $CeVO_4$ nanostructure that was studied in the previous research work [33], a nanocomposite sample was created and the performance of both samples (pure oxide and nanocomposite) was measured and compared at 15 cycles. Each cycle contains adsorption and desorption. In the case of both nanostructured samples, it is observed that the adsorption and desorption cycles can boost. In the case of

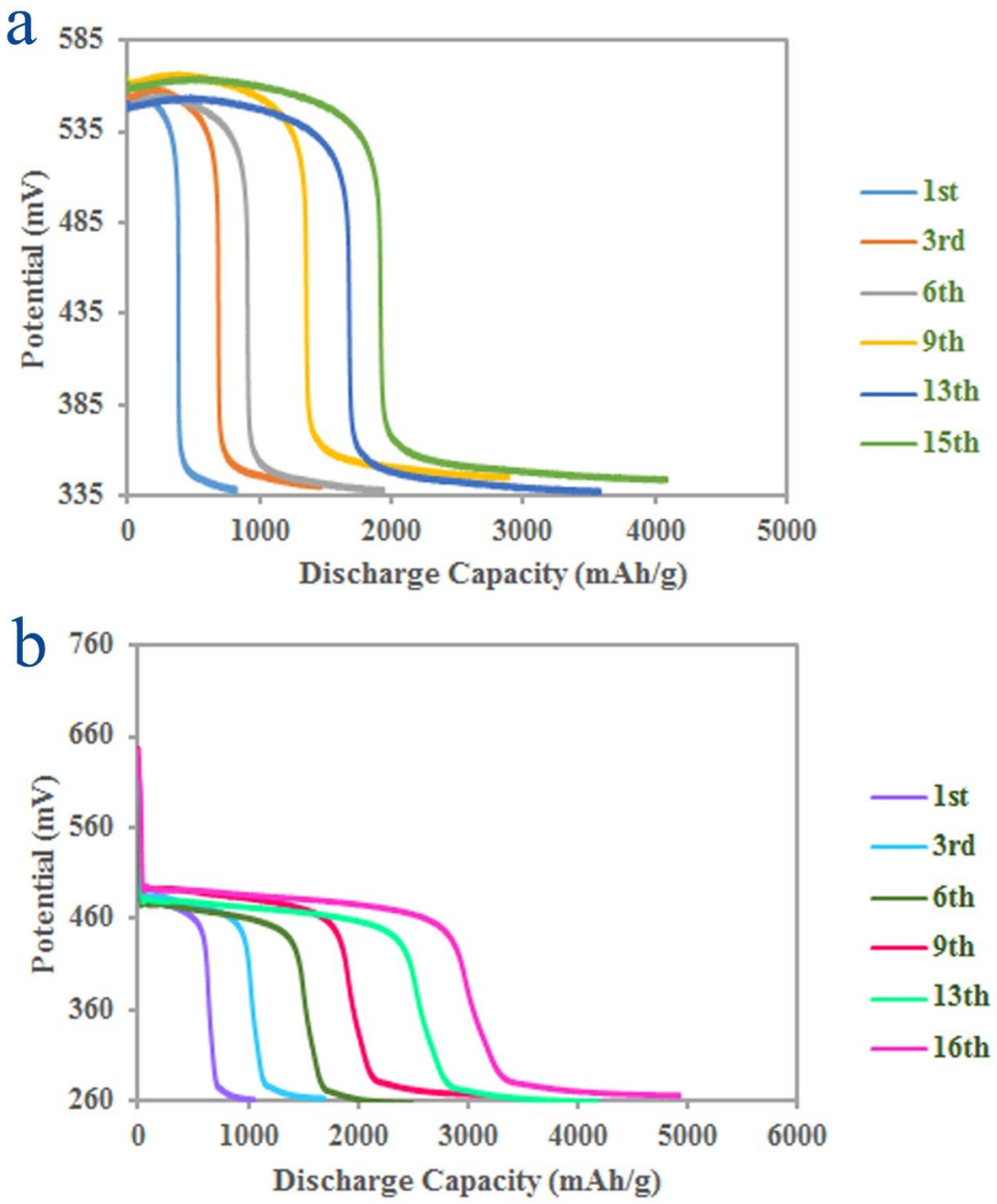

Fig. 9. Discharge profiles for (a) pure oxide nanostructure and (b) the as-synthesized $CeVO_4$/rGO nanocomposite.

nanocomposite sample, however, in all cycles, the measured adsorption capacity is greater than the adsorption capacity of the pure oxide sample (see Figs. 9 and 10). Pure oxide sample capacity can only be enhanced to about 4087 mAh/g after 15 adsorption-desorption cycles, while in the nanocomposite sample, capacity from 1051 mAh/g in the first cycle can reach about 4929 mAh/g in the 15th cycle. Adding reduced graphene oxide here improved the hydrogen storage capacity. As mentioned earlier, the BET outcomes showed that the specific surface area enhanced with the addition of reduced graphene oxide (see Fig. 5). In other words, the specific surface area of the

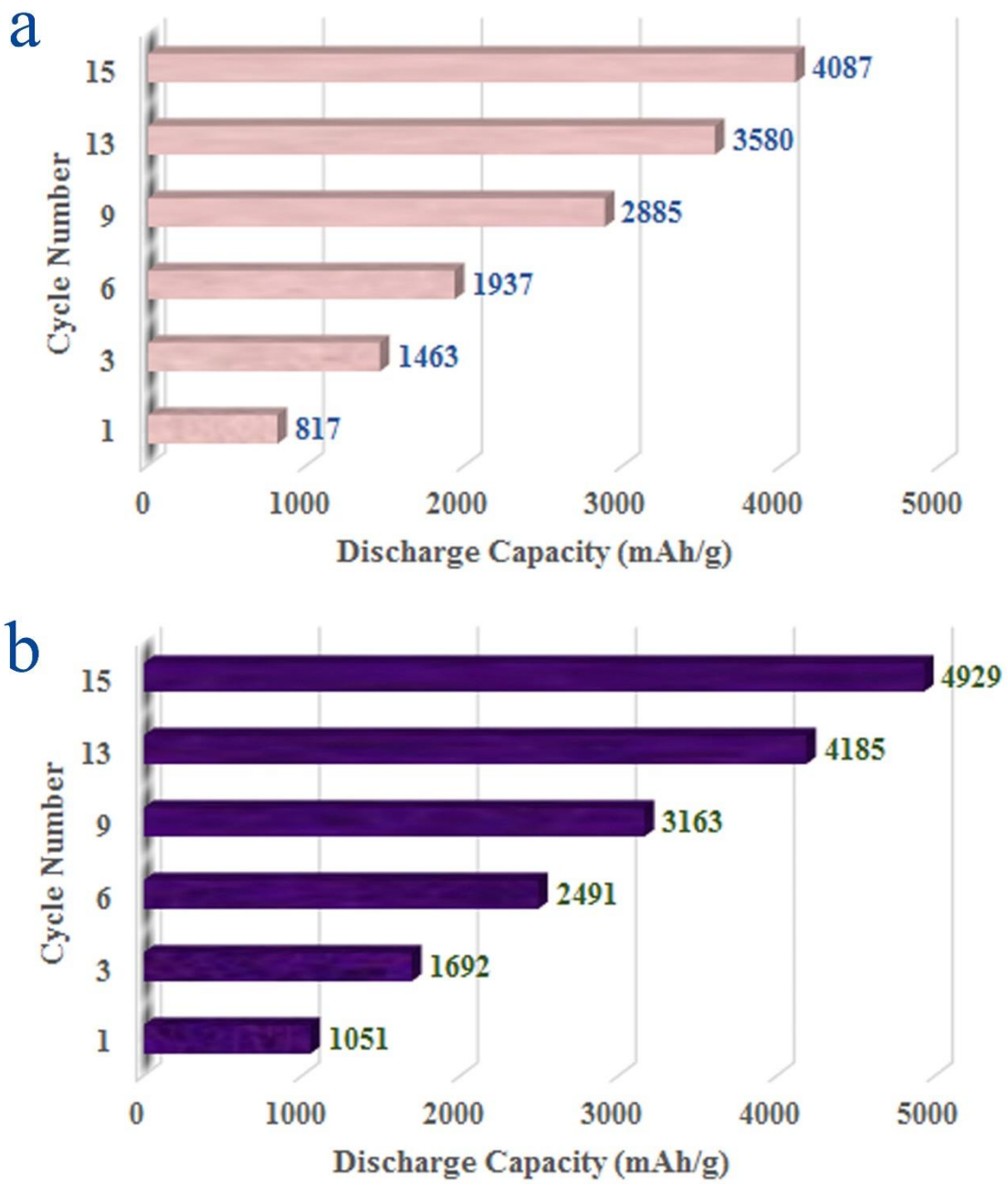

Fig. 10. Cycling performance of (a) pure oxide nanostructure and (b) the as-synthesized $CeVO_4$/rGO nanocomposite.

pure oxide nanostructure is lower than that of the nanocomposite sample. Previous studies have demonstrated that having proper porosity and great specific area can play a very positive role in boosting the electrochemical storage capacity of hydrogen [16]. So, it seems that adding reduced graphene oxide, and as a result, the preparation of nanocomposite sample can be a beneficial approach to achieve better performance in electrochemical hydrogen storage. It is worth mentioning that the copper substrate without the presence of prepared nanostructures as electrode compounds exhibited a negligible capacity. This means that both synthesized nanostructures have a substantial effect on the obtained hydrogen storage capacities [46, 47].

In addition, the reason for the enhancement in discharge capacity with the increment in the number of adsorption-desorption cycles can be said to be the creation of more new sites for hydrogen adsorption and desorption in the working electrode [48]. Fig. 11 displays the last charge profiles of the both samples (pure oxide and nanocomposite) at room temperature. The appearance of different plateaus in the charge profile related to both nanostructured samples

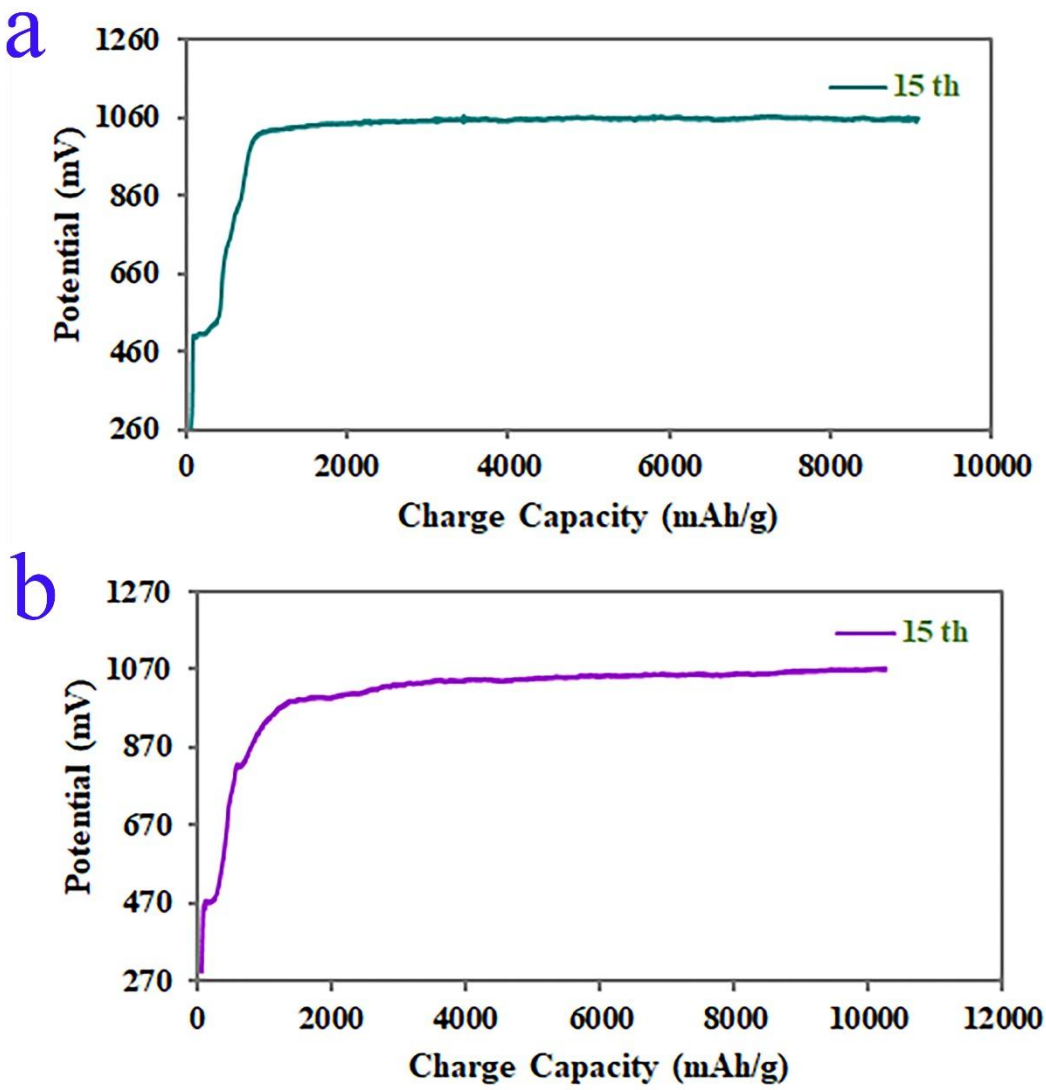

Fig. 11. The last charge profiles for (a) pure oxide nanostructure and (b) the as-synthesized $CeVO_4$/rGO nanocomposite.

can demonstrate the existence of diverse sites for hydrogen absorption in the structure of these nanomaterials [49]. The above outcomes illustrate that the positive effect of adding reduced graphene oxide can provide alternative insights to produce nanocomposites with favorable structural and morphological characteristics for green energy storage uses very efficiently.

CONCLUSION

In this study, the $CeVO_4$/rGO nanocomposite was fabricated by a one-pot sonochemical approach utilizing $Ce(NO_3)_3{\cdot}6H_2O$), NH_4VO_3, and GO as reactants and hydrazine as both reducing agent and OH^- source. $CeVO_4$/rGO nanocomposite was dried for 10 hours at 80 °C and then identified by EDS, FT-IR, XRD, BET, and FESEM analyses. The characterization results indicate that rod-like $CeVO_4$ nanoparticles were formed on the reduced graphene oxide sheets. The results show the positive effect of adding reduced graphene oxide. This provides new insight into efficiently producing nanocomposites with favorable structural and morphological properties for green energy storage applications. Finally, the nanocomposite obtained by the chrono-potentiometric method was used for the electrochemical hydrogen storage. The hydrogen storage capacity was calculated to be 4929 mAh/g. The focus of current and future research is on the modification of existing materials and the development of new materials.

ACKNOWLEDGMENT

The authors would like to thank Semnan University Research Council and University of Bonab for the financial support of this work.

CONFLICT OF INTEREST

The authors declare that there is no conflict of interests regarding the publication of this manuscript.

REFERENCES

1. Zamehrian M, Sedaee B. Underground hydrogen storage in a partially depleted gas condensate reservoir: Influence of cushion gas. Journal of Petroleum Science and Engineering. 2022;212:110304.
2. Heinemann N, Scafidi J, Pickup G, Thaysen EM, Hassanpouryouzband A, Wilkinson M, et al. Hydrogen storage in saline aquifers: The role of cushion gas for injection and production. Int J Hydrogen Energy. 2021;46(79):39284-39296.
3. Deveci M. Site selection for hydrogen underground storage using interval type-2 hesitant fuzzy sets. Int J Hydrogen Energy. 2018;43(19):9353-9368.
4. Muhammed NS, Haq B, Al Shehri D, Al-Ahmed A, Rahman MM, Zaman E. A review on underground hydrogen storage: Insight into geological sites, influencing factors and future outlook. Energy Reports. 2022;8:461-499.
5. Meda US, Bhat N, Pandey A, Subramanya KN, Lourdu Antony Raj MA. Challenges associated with hydrogen storage systems due to the hydrogen embrittlement of high strength steels. Int J Hydrogen Energy. 2023;48(47):17894-17913.
6. Sainz-Garcia A, Abarca E, Rubi V, Grandia F. Assessment of feasible strategies for seasonal underground hydrogen storage in a saline aquifer. Int J Hydrogen Energy. 2017;42(26):16657-16666.
7. Zamehrian M, Sedaee B. Underground hydrogen storage in a naturally fractured gas reservoir: The role of fracture. Int J Hydrogen Energy. 2022;47(93):39606-39618.
8. Valian M, Mahdi MA, Jasim LS, Salavati-Niasari M. Significantly improved electrochemical hydrogen storage accomplishment promoted by novel $Li_{0.35}La_{0.55}TiO_3$/rGO nanocomposite. Journal of Energy Storage. 2024;84:110862.
9. Ball M, Weeda M. The hydrogen economy – Vision or reality? 1 1This paper is also published as Chapter 11 'The hydrogen economy – vision or reality?' in Compendium of Hydrogen Energy Volume 4: Hydrogen Use, Safety and the Hydrogen Economy, Edited by Michael Ball, Angelo Basile and T. Nejat Veziroglu, published by Elsevier in 2015, ISBN: 978-1-78242-364-5. Int J Hydrogen Energy. 2015;40(25):7903-7919.
10. Wu Y, Liu X, Bai X, Wu W. Ultrasonic-assisted preparation of ultrafine Pd nanocatalysts loaded on Cl−-intercalated MgAl layered double hydroxides for the catalytic dehydrogenation of dodecahydro-N-ethylcarbazole. Ultrason Sonochem. 2022;88:106097.
11. Dehane A, Merouani S, Chibani A, Hamdaoui O. Clean hydrogen production by ultrasound (sonochemistry): The effect of noble gases. Current Research in Green and Sustainable Chemistry. 2022;5:100288.
12. Zonarsaghar A, Mousavi-Kamazani M, Zinatloo-Ajabshir S. Hydrothermal synthesis of $CeVO_4$ nanostructures with different morphologies for electrochemical hydrogen storage. Ceram Int. 2021;47(24):35248-35259.
13. Navaid HB, Emadi H, Watson M. A comprehensive literature review on the challenges associated with underground hydrogen storage. Int J Hydrogen Energy. 2023;48(28):10603-10635.
14. Das D. Hydrogen production by biological processes: a survey of literature. Int J Hydrogen Energy. 2001;26(1):13-28.
15. Gholami T, Pirsaheb M. Review on effective parameters in electrochemical hydrogen storage. Int J Hydrogen Energy. 2021;46(1):783-795.
16. Kaur M, Pal K. Review on hydrogen storage materials and methods from an electrochemical viewpoint. Journal of Energy Storage. 2019;23:234-249.
17. Zivar D, Kumar S, Foroozesh J. Underground hydrogen storage: A comprehensive review. Int J Hydrogen Energy. 2021;46(45):23436-23462.
18. Lewandowska-Śmierzchalska J, Tarkowski R, Uliasz-Misiak B. Screening and ranking framework for underground hydrogen storage site selection in Poland. Int J Hydrogen Energy. 2018;43(9):4401-4414.
19. Zohrabian A, Mansouri Majoumerd M, Soltanieh M, Sattari S. Techno-economic evaluation of an integrated hydrogen and power co-generation system with CO_2 capture. International

Journal of Greenhouse Gas Control. 2016;44:94-103.
20. Bosu S, Rajamohan N. Recent advancements in hydrogen storage - Comparative review on methods, operating conditions and challenges. Int J Hydrogen Energy. 2024;52:352-370.
21. Najjar YSH. Hydrogen safety: The road toward green technology. Int J Hydrogen Energy. 2013;38(25):10716-10728.
22. Mouli-Castillo J, Heinemann N, Edlmann K. Mapping geological hydrogen storage capacity and regional heating demands: An applied UK case study. Applied Energy. 2021;283:116348.
23. Roy P, Das N. Ultrasonic assisted synthesis of Bikitaite zeolite: A potential material for hydrogen storage application. Ultrason Sonochem. 2017;36:466-473.
24. Cho Y, Cho H, Cho ES. Nanointerface Engineering of Metal Hydrides for Advanced Hydrogen Storage. Chem Mater. 2023;35(2):366-385.
25. Eftekhari A, Fang B. Electrochemical hydrogen storage: Opportunities for fuel storage, batteries, fuel cells, and supercapacitors. Int J Hydrogen Energy. 2017;42(40):25143-25165.
26. Wan H, Yang X, Zhou S, Ran L, Lu Y, Chen Ya, et al. Enhancing hydrogen storage properties of MgH2 using FeCoNiCrMn high entropy alloy catalysts. Journal of Materials Science and Technology. 2023;149:88-98.
27. Chandra Muduli R, Kale P. Silicon nanostructures for solid-state hydrogen storage: A review. Int J Hydrogen Energy. 2023;48(4):1401-1439.
28. Kumar A, Singh AK, Tomar M, Gupta V, Kumar P, Singh K. Electromagnetic interference shielding performance of lightweight $NiFe_2O_4$/rGO nanocomposite in X- band frequency range. Ceram Int. 2020;46(10):15473-15481.
29. Guemou S, Zhang L, Li S, Jiang Y, Zhong T, Lu Z, et al. Exceptional catalytic effect of novel rGO-supported Ni-Nb nanocomposite on the hydrogen storage properties of MgH_2. Journal of Materials Science & Technology. 2024;172:83-93.
30. Karami M, Ghanbari M, Amiri O, Ghiyasiyan-Arani M, Salavati-Niasari M. Sonochemical synthesis, characterization and investigation of the electrochemical hydrogen storage properties of $TlPbI_3$/$Tl4PbI_6$ nanocomposite. Int J Hydrogen Energy. 2021;46(9):6648-6658.
31. Cao N, Zhang Y. Study of Reduced Graphene Oxide Preparation by Hummers' Method and Related Characterization. Journal of Nanomaterials. 2015;2015(1).
32. Rezayeenik M, Mousavi-Kamazani M, Zinatloo-Ajabshir S. $CeVO_4$/rGO nanocomposite: facile hydrothermal synthesis, characterization, and electrochemical hydrogen storage. Appl Phys A. 2022;129(1).
33. Zonarsaghar A, Mousavi-Kamazani M, Zinatloo-Ajabshir S. Sonochemical synthesis of $CeVO_4$ nanoparticles for electrochemical hydrogen storage. Int J Hydrogen Energy. 2022;47(8):5403-5417.
34. Mousavi-Kamazani M, Alizadeh S, Ansari F, Salavati-Niasari M. A controllable hydrothermal method to prepare $La(OH)_3$ nanorods using new precursors. Journal of Rare Earths. 2015;33(4):425-431.
35. Anju, Yadav RS, Pötschke P, Pionteck J, Krause B, Kuřitka I, et al. $Cu_xCo_{1-x}Fe_2O_4$ (x = 0.33, 0.67, 1) Spinel Ferrite Nanoparticles Based Thermoplastic Polyurethane Nanocomposites with Reduced Graphene Oxide for Highly Efficient Electromagnetic Interference Shielding. Int J Mol Sci. 2022;23(5):2610.
36. Ambroz F, Macdonald TJ, Martis V, Parkin IP. Evaluation of the BET Theory for the Characterization of Meso and Microporous MOFs. Small Methods. 2018;2(11).
37. Kaur M, Pal K. Potential electrochemical hydrogen storage in nickel and cobalt nanoparticles-induced zirconia-graphene nanocomposite. Journal of Materials Science: Materials in Electronics. 2020;31(13):10903-10911.
38. Monsef R, Ghiyasiyan-Arani M, Salavati-Niasari M. Design of Magnetically Recyclable Ternary Fe_2O_3/$EuVO_4$/g-C_3N_4 Nanocomposites for Photocatalytic and Electrochemical Hydrogen Storage. ACS Applied Energy Materials. 2021;4(1):680-695.
39. Alothman Z. A Review: Fundamental Aspects of Silicate Mesoporous Materials. Materials. 2012;5(12):2874-2902.
40. Sangsefidi FS, Salavati-Niasari M, Varshoy S, Shabani-Nooshabadi M. Investigation of Mn2O3 as impurity on the electrochemical hydrogen storage performance of MnO_2CeO_2 nanocomposites. Int J Hydrogen Energy. 2017;42(47):28473-28484.
41. Ding J, Liu X, Wang M, Liu Q, Sun T, Jiang G, et al. Controlled synthesis of $CeVO_4$ hierarchical hollow microspheres with tunable hollowness and their efficient photocatalytic activity. CrystEngComm. 2018;20(31):4499-4505.
42. Karkeh-Abadi F, Ghiyasiyan-Arani M, Salavati-Niasari M. Sonochemical synthesized $BaMoO_4$/ZnO nanocomposites as electrode materials: A comparative study on GO and GQD employed in hydrogen storage. Ultrason Sonochem. 2022;90:106167.
43. Pirsaheb M, Gholami T, Seifi H, Yousif QA, Salavati-Niasari M. Investigate of electrochemical hydrogen storage and coulombic efficiency of $NiAl_2O_4$/NiO synthesized by cationic, anionic and polymeric surfactants: Green synthesis and characterization. Int J Hydrogen Energy. 2022;47(82):34994-35002.
44. Pirsaheb M, Gholami T, Dawi EA, Majdi HS, Hashim FS, Seifi H, et al. Green synthesis and characterization of SnO_2, CuO, Fe_2O_3/activated carbon nanocomposites and their application in electrochemical hydrogen storage. Int J Hydrogen Energy. 2023;48(61):23594-23606.
45. Jurewicz K, Frackowiak E, Béguin F. Towards the mechanism of electrochemical hydrogen storage in nanostructured carbon materials. Appl Phys A. 2004;78(7):981-987.
46. Sangsefidi FS, Salavati-Niasari M. Fe_2O_3–CeO_2 Ceramic Nanocomposite Oxide: Characterization and Investigation of the Effect of Morphology on Its Electrochemical Hydrogen Storage Capacity. ACS Applied Energy Materials. 2018;1(9):4840-4848.
47. Yousaf S, Zulfiqar S, Shahid M, Jamil A, Shakir I, Agboola PO, et al. Electrochemical energy storage properties studies of $Cu_{0.2}Ni_{0.8}O$-Reduced graphene oxide nano-hybrids. Ceram Int. 2020;46(9):14304-14310.
48. Gholami T, Salavati-Niasari M, Varshoy S. Electrochemical hydrogen storage capacity and optical properties of $NiAl_2O_4$/NiO nanocomposite synthesized by green method. Int J Hydrogen Energy. 2017;42(8):5235-5245.
49. Salehabadi A, Salavati-Niasari M, Gholami T. Green and facial combustion synthesis of $Sr_3Al_2O_6$ nanostructures; a potential electrochemical hydrogen storage material. Journal of Cleaner Production. 2018;171:1-9.